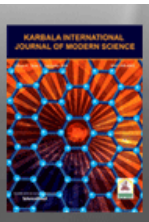

Karbala International Journal of Modern Science

Volume 11 | Issue 3 Article 10

Psilostachyin B as Potential Immune Checkpoint Inhibitor Targeting CTLA-4 and PD-L1 in the Development of Cancer Immunotherapy: A Computational Investigation

Moh Dliyauddin
Biology Department, Faculty of Mathematics and Natural Sciences, Brawijaya University, 65145 Malang, Indonesia;

Nabila Shafa Yumna Salsabila
Biology Department, Faculty of Mathematics and Natural Sciences, Brawijaya University, 65145 Malang, Indonesia

Noviana Dwi Lestari
Medical Education Study Program, Faculty of Medicine, Muhammadiyah Malang University, 65145 Malang, Indonesia

Sapti Puspitarini
Department of Natural Science, Faculty of Mathematics and Natural Science, Universitas Negeri Surabaya, Surabaya, 60231, Indonesia

Mansur Ibrahim
Faculty of Pharmacy, Megarezky University, Makassar 90234, Indonesia

See next page for additional authors

Follow this and additional works at: https://kijoms.uokerbala.edu.iq/home

 Part of the Biology Commons, Chemistry Commons, Computer Sciences Commons, and the Physics Commons

Recommended Citation

Dliyauddin, Moh; Salsabila, Nabila Shafa Yumna; Lestari, Noviana Dwi; Puspitarini, Sapti; Ibrahim, Mansur; Rahayu, Sri; Djati, Muhammad Sasmito; and Rifa'i, Muhaimin (2025) "Psilostachyin B as Potential Immune Checkpoint Inhibitor Targeting CTLA-4 and PD-L1 in the Development of Cancer Immunotherapy: A Computational Investigation," *Karbala International Journal of Modern Science*: Vol. 11 : Iss. 3 , Article 10.
Available at: https://doi.org/10.33640/2405-609X.3417

This Research Paper is brought to you for free and open access by Karbala International Journal of Modern Science. It has been accepted for inclusion in Karbala International Journal of Modern Science by an authorized editor of Karbala International Journal of Modern Science. For more information, please contact abdulateef1962@gmail.com.

University of Kerbala

Psilostachyin B as Potential Immune Checkpoint Inhibitor Targeting CTLA-4 and PD-L1 in the Development of Cancer Immunotherapy: A Computational Investigation

Abstract

Immunotherapy is a promising treatment approach by targeting immune checkpoints such as CTLA-4 and PD-L1 to overcome cancer progression. The utilization of *Curcuma longa* and *Phyllanthus niruri* as potential immune checkpoint inhibitors offers an alternative cancer therapy. Computational analyses including molecular docking and molecular dynamics with validation using Molecular Mechanics/ Poisson-Boltzmann Surface Area (MM-PBSA), Dynamic Cross-Correlation Matrix (DCCM), and Principal Component Analysis (PCA), were performed in this study. Results show that Psilostachyin B is the most promising inhibitor candidate against CTLA-4 and PD-L1, with binding affinity values of -6.9 and -6.8 kcal/ mol, respectively. Molecular dynamics simulation results indicated that Psilostachyin B exhibited greater stability than the native ligand, with RMSD values remaining below 3 Å for the ligand–complex on CTLA-4 and PD-L1 over 40 ns and 20 ns, respectively. These findings were further supported by favorable binding free energy values from MM-PBSA calculations, as well as positive correlations observed in DCCM and stable conformational profiles revealed by PCA. Moreover, PPI analysis showed that Psilostachyin B interacts with various key cancer-related proteins based on Gene Ontology annotations and KEGG pathway analysis. Psilostachyin B is a promising drug candidate with favorable drug-likeness, high predicted antineoplastic activity (Pa 95%), and efficient membrane permeability. This computational investigation highlights the potential of Psilostachyin B as a novel immune checkpoint inhibitor targeting CTLA-4 and PD-L1, two key regulators involved in modulating the tumor microenvironment and enhancing immune responses. Future studies through in vitro and in vivo studies are necessary to evaluate its efficacy before clinical application.

Keywords

C. longa; P. niruri; Psilostachyin B; CTLA-4; PD-L1; Immune Checkpoint Inhibitor

Creative Commons License

This work is licensed under a Creative Commons Attribution-Noncommercial-No Derivative Works 4.0 License.

Authors

Moh Dliyauddin, Nabila Shafa Yumna Salsabila, Noviana Dwi Lestari, Sapti Puspitarini, Mansur Ibrahim, Sri Rahayu, Muhammad Sasmito Djati, and Muhaimin Rifa'i

This research paper is available in Karbala International Journal of Modern Science: https://kijoms.uokerbala.edu.iq/home/vol11/iss3/10

RESEARCH PAPER

Psilostachyin B as Potential Immune Checkpoint Inhibitor Targeting CTLA-4 and PD-L1 in the Development of Cancer Immunotherapy: A Computational Investigation

Moh Dliyauddin [a], Nabila S.Y. Salsabila [a], Noviana D. Lestari [b], Sapti Puspitarini [c], Mansur Ibrahim [d], Sri Rahayu [a], Muhammad S. Djati [a], Muhaimin Rifa'i [a,*]

[a] Biology Department, Faculty of Mathematics and Natural Sciences, Brawijaya University, 65145 Malang, Indonesia
[b] Medical Education Study Program, Faculty of Medicine, Muhammadiyah Malang University, 65145 Malang, Indonesia
[c] Department of Natural Science, Faculty of Mathematics and Natural Science, Universitas Negeri Surabaya, Surabaya 60231, Indonesia
[d] Faculty of Pharmacy, Megarezky University, Makassar 90234, Indonesia

Abstract

Immunotherapy is a promising treatment approach by targeting immune checkpoints such as CTLA-4 and PD-L1 to overcome cancer progression. The utilization of *Curcuma longa* and *Phyllanthus niruri* as potential immune checkpoint inhibitors offers an alternative cancer therapy. Computational analyses including molecular docking and molecular dynamics with validation using Molecular Mechanics/Poisson-Boltzmann Surface Area (MM-PBSA), Dynamic Cross-Correlation Matrix (DCCM), and Principal Component Analysis (PCA), were performed in this study. Results show that Psilostachyin B is the most promising inhibitor candidate against CTLA-4 and PD-L1, with binding affinity values of −6.9 and −6.8 kcal/mol, respectively. Molecular dynamics simulation results indicated that Psilostachyin B exhibited greater stability than the native ligand, with RMSD values remaining below 3 Å for the ligand−complex on CTLA-4 and PD-L1 over 40 ns and 20 ns, respectively. These findings were further supported by favorable binding free energy values from MM-PBSA calculations, as well as positive correlations observed in DCCM and stable conformational profiles revealed by PCA. Moreover, PPI analysis showed that Psilostachyin B interacts with various key cancer-related proteins based on Gene Ontology annotations and KEGG pathway analysis. Psilostachyin B is a promising drug candidate with favorable drug-likeness, high predicted antineoplastic activity (Pa 95 %), and efficient membrane permeability. This computational investigation highlights the potential of Psilostachyin B as a novel immune checkpoint inhibitor targeting CTLA-4 and PD-L1, two key regulators involved in modulating the tumor microenvironment and enhancing immune responses. Future studies through in vitro and in vivo studies are necessary to evaluate its efficacy before clinical application.

Keywords: *C. longa*, *P. niruri*, Psilostachyin B, CTLA-4, PD-L1, Immune checkpoint inhibitor

1. Introduction

Cancer is a leading cause of death worldwide, with rising incidence and treatment resistance. Despite advances in surgery, chemotherapy, and radiation, many cancers evade immune detection, leading to recurrence. Cancer cells have the ability to influence the tumor microenvironment (TME), which is a key factor in evading the body's defense mechanism [1]. One of the strategies cancer cells used to modify the TME is by creating an immunosuppressive environment, suppressing the immune system's ability to fight cancer cells and promoting a pro-tumor environment [2]. Therefore, understanding how cancer interacts with the immune system has become a critical focus in modern

Received 12 March 2025; revised 18 June 2025; accepted 22 June 2025.
Available online 16 July 2025

* Corresponding author.
E-mail address: immunobiology@ub.ac.id (M. Rifa'i).

https://doi.org/10.33640/2405-609X.3417
2405-609X/© 2025 University of Kerbala. This is an open access article under the CC-BY-NC-ND license (http://creativecommons.org/licenses/by-nc-nd/4.0/).

oncology. One of the main mechanisms involved is the upregulation of immune checkpoint molecules such as Programmed Death-Ligand 1 (PD-L1) on the surface of cancer cells, which is effectively preventing T cell attacks [3]. In addition, the immunosuppressive mechanism is further reinforced through the influence of other checkpoint proteins, such as Cytotoxic T-lymphocyte-associated protein 4 (CTLA-4), which plays a role in inhibiting the initial activation of T cells [4]. Within the TME, the immune response to cancer cells triggers the recruitment and activation of immune cells that support tumor growth, such as Regulatory T cells (Tregs), which suppress the antitumor immune response [5]. This allows cancer cells to continue growing and developing without being detected or destroyed by the immune system.

Immunotherapy is a widely used treatment method for combating various types of cancer. One of the immunotherapy approaches involves regulating the immune system's mechanism in combating tumor cells through immune checkpoint inhibitors [6]. PD-L1 is a ligand that interacts with Programmed Death-1 (PD-1) receptors found on T cells. When PD-L1 is expressed by cancer cells, it binds to PD-1 on T cells then a negative signal is transmitted, leading to a reduction in effector activity and T cell proliferation [7]. This mechanism inhibits the immune system's ability to recognize and destroy cancer cells. In the tumor microenvironment (TME), cancer cells and surrounding components often exploit CTLA-4 expression on regulatory T cells (Tregs) to further suppress immune activity [8]. The activation of Tregs in the TME can inhibit effector T cell activation through various biological mechanisms, such as the secretion of immunosuppressive cytokines like IL-10 and TGF-β [9]. The activation of PD-L1 and CTLA-4 has a synergistic effect in helping cancer cells evade immune attack. CTLA-4 primarily functions during the early stages of T cell activation in lymphoid organs, whereas PD-L1 operates at the effector stage within the tumor microenvironment. The combination of these two mechanisms significantly weakens the immune response, allowing more aggressive tumors to grow [10].

In several clinical studies, the combination of PD-1/PD-L1 and CTLA-4 therapies has demonstrated greater efficacy than monotherapy. One example is the combination of *nivolumab* (anti-PD-1) and *ipilimumab* (anti-CTLA-4), which has been shown to enhance immune responses against various types of cancer [11]. Immune checkpoint inhibitors work by removing barriers to T cell activation and effector function, allowing the immune system to recognize and eliminate cancer cells more effectively [12]. Anti-PD-L1 and anti-CTLA-4 are key targets in cancer immunotherapy due to their ability to amplify the immune response against cancer cells. The mechanism of action of the anti-PD-L1 and anti-CTLA-4 combination lies in its ability to eliminate obstacles to T cell activation and effector function, thereby enhancing immune recognition and destruction of cancer cells [13]. Moreover, the inhibition of PD-1/PD-L1 and CTLA-4 not only counteracts the immune escape mechanisms employed by cancer cells but also strengthens the adaptive immune response. Therefore, these two targets are considered crucial therapeutic approaches in cancer immunotherapy development, offering new hope for improving treatment outcomes in cancer patients [14].

In the development of targeted immunotherapies, herbal medicine has gained attention due to its multifaceted pharmacological properties and potential to produce superior therapeutic outcomes compared to synthetic drugs. *Curcuma longa* (turmeric) and *Phyllanthus niruri* (meniran) are two herbs known for their various health benefits, including anti-cancer and anti-diabetic properties [15,16]. Additionally, *C. longa* is well recognized for its strong antioxidant properties [17], while *P. niruri* functions as an immunostimulant that enhances the activity of cytotoxic T cells, which play a crucial role in destroying cancer cells [18]. The potential role of these herbs compounds in modulating the immune system and exhibiting anticancer activity through the regulation of immune checkpoints such as PD-L1 and CTLA-4 using in silico approaches remains limited.

In this study, an in silico approach combining molecular docking and molecular dynamics simulations was employed to investigate the interaction profiles of selected phytochemicals with the immune checkpoint proteins PD-L1 and CTLA-4, which are critical regulators of tumor-induced immune suppression. This computational strategy enabled the prediction of binding affinities and conformational stability, providing mechanistic insights into the inhibitory potential of these compounds on immune checkpoint signaling pathways [19]. The integrated modeling framework facilitated the efficient screening and prioritization of bioactive candidates with favorable interaction profiles, establishing a strong rationale for downstream experimental validation. By targeting molecular pathways associated with immune evasion, this study supports the development of novel candidate immunotherapeutic agents derived from medicinal plants, potentially associated with limited side effects. This study aims to contribute to ongoing

efforts to expand immunomodulatory strategies against cancer through nature-inspired drug discovery.

2. Methods

2.1. Identification of bioactive compound using LCHRMS analysis

The formulation of *C. longa* and *P. niruri* (1:1 ratio) was obtained from Ismut Fitomedika Indonesia (IFI). The bioactive compounds of *C. longa* and *P. niruri* were analyzed using the Thermo Scientific Ultimate 3000 RSLCnano-Q Exactive™ Plus Hybrid Quadrupole-Orbitrap™ Mass Spectrometer at the Laboratorium Riset Terpadu (LRT), Brawijaya University, Indonesia. The prepared samples were placed in an autosampler and injected into an LC-HRMS system. Data processing was conducted using Compound Discoverer version 3.2 (Thermo Scientific) with the mzCloud MS/MS Library for analysis [20]. Compounds with a BestMatch value exceeding 85 % similarity were selected for further analysis. The selected compounds were compiled into 3D structures and its 3D-SDF file format and canonical SMILES were retrieved from the PubChem database for further study [21].

2.2. Molecular docking screening

Molecular docking in this study was used as a screening method to identify potential compounds that can interact with CTLA-4 and PD-L1 target proteins (Table 1). The target proteins used were PD-L1 (PDB ID: 5J89) and CTLA-4 (PDB ID: 1I8L) [22,23]. The native ligands used were the PD-L1 inhibitor BMS-202 (PubChem ID: 117951478) and the CTLA-4 inhibitor 2-acetamido-2-deoxy-beta-D-glucopyranose (PubChem ID: 24139). Simulations were performed using AutoDock Vina in PyRx. Two controls including a drug control (Doxorubicin) and a native ligand were used in this study to compare the effectiveness and validity of the test compound's interaction with the target protein.

Active site predictions for the target proteins were obtained from binding sites identified through blind docking with the native ligands using AutoDock Vina [24]. Molecular docking results were visualized using Discovery Studio 2019 software. Molecular tethering simulations were performed by energetically binding the bioactive compound to the target protein.

Potential compounds with the best binding energy values were selected for molecular dynamics analysis. Molecular dynamics simulations were performed using Yet Another Scientific Artificial Reality Application (YASARA) software with the AMBER14 force field [25]. System parameters were set to mimic the physiological environment of cells, including a temperature of 37 °C, pH of 7.4, pressure of 1 atm, and a salt concentration of 0.9 %, with a simulation duration of 100 ns. The temperature of 310 K closely reflects human physiological conditions, and it's commonly used in molecular dynamics (MD) simulations to mimic the human body environment. The main programs used included md_run to execute the simulation, md_analyze to evaluate the Root Mean Square Deviation (RMSD), and md_bindingenergy to analyze the binding energy of protein-ligand complexes. The binding energy in this context is calculated using the Molecular Mechanics/Poisson-Boltzmann Surface Area (MM-PBSA) method. By integrating the analysis of various parameters derived from molecular dynamics (MD) simulations, the prediction of a compound as a potential drug candidate can be performed with greater accuracy [26]. The molecular mechanics Poisson-Boltzmann surface area (MM/PBSA) method was applied using the YASARA macro, specifically md_analyzebindenergy.mcr, to conduct binding free energy calculations considering the solvation of the ligand, complex, and free protein, among others [27].

To analyze the dynamical behavior in the conformational space, RStudio was used to perform Dynamic Cross-Correlation Matrix (DCCM) and Principal Component Analysis (PCA). During a 100 ns MD simulation, a DCCM was constructed based

Table 1. Protein preparation in molecular docking.

No	Protein	PDB ID	Active Site Prediction	Inhibitor	Grid Center
1	PD-L1	5j89 (Chain: B)	TYR 32, SER80, ARG84, ASP103, GLN107, LEU106, LYS 105, HIS140, GLU139	BMS-202 (PubChem ID: 117951478)	Center = X: 7.0223, Y: 1.7972, Z: 162.9474 Dimensions (A) = X: 23.0904, Y: 27.4865, Z: 22.9468
2	CTLA-4	1I8L (Chain: A)	VAL104, GLU77, PRO74, PHE134, PRO135, ASP107, LYS105, LEU189, ALA106	2-acetamido-2-deoxy-beta-D-glucopyranose (PubChem ID: 24139)	Center = X: 12.2041, Y: 87.5202, Z: 157.2734 Dimensions (A) = X: 25.0000, Y: 26.3347, Z: 27.5026

on all Cα atoms of the CTLA4 and PD-L1 complex to examine domain correlations. PCA was applied to the same 100 ns simulation to capture the global motions of the trajectories. For the PCA, a covariance matrix was generated as described. Data analysis was performed using PAST4 and RStudio, employing the "mktrj.pca" function from the Bio3D package for MD trajectory analysis [28].

2.3. Protein–protein interaction (PPI) network and functional annotation construction

The target proteins of Psilostachyin B compounds were obtained from the SWISS Target Prediction database (http://www.swisstargetprediction.ch/) or STITCH (http://stitch.embl.de/). The most promising target proteins were selected based on the results of potential compound screening. Indirect targets of each active compound were retrieved from the STRING web server (https://string-db.org/) by inputting the identified target proteins. All obtained results were then integrated and visualized using Cytoscape 3.10.3 software [29].

All proteins obtained from the PPI network construction were input into the DAVID web server (https://davidbioinformatics.nih.gov/). Functional annotation was performed using the Gene Ontology (GO) and KEGG pathway databases, with a focus on biological mechanisms related to immune response and cancer apoptosis [30].

2.4. Drug-likeness, bioactivity, and membrane permeability of potential compound

Potential compounds found in the *C. longa* and *P. niruri* herbs were subjected to drug similarity screening using the SWISS ADME web server (https://www.swissadme.ch/) [31]. The bioavailability of each compound was predicted using the PASS Online web server (http://www.way2drug.com/passonline), in which the probable activity (Pa) value was assessed based on various biological activities [32]. Furthermore, the ability of each compound to penetrate the lipid bilayer of cell membranes was analyzed using the PerMM server (https://permm.phar.umich.edu). The PDB files of the compounds were uploaded, and physiological conditions were set at 310 K and pH 7.4. The energy transfer values of each compound were then compared and visualized in 3D using Discovery Studio 2019 [25,33].

3. Results and discussion

3.1. Bioactive compound

Based on LC-HRMS analysis, at least 16 compounds were found with 85 best matches as can be seen in Table 2. The molecular weights of the compounds contained in the combination of *C. longa* and *P. niruri* were in the range of 71–368 g/mol, in which choline had the lowest and curcumin had the highest molecular weight. Molecular weight is a critical parameter in medical biochemistry as it influences a compound's ability to cross biological membranes, interact with cellular receptors, and modulate metabolic pathways [34]. In this context, low molecular weight compounds, such as choline (71 g/mol), potentially have better penetration ability into tissues, including the central nervous system. In contrast, higher molecular weight compounds, such as curcumin (368 g/mol), may require structural

Table 2. Bioactive compounds in C. longa *and* P. niruri *from library LC-HRMS analysis.*

No	Name	Formula	Molecular Weight (MW) (g/mol)	Retention Time (RT) [min]	Area (Max.)	mzCloud Best Match
1	Trigonelline	$C_7 H_7 N O_2$	137.04	0.883	28126358.41	93.1
2	Erucamide	$C_{22} H_{43} N O$	337.33	66.39	205633.5199	92.7
3	DL-Carnitine	$C_7 H_{15} N O_3$	161.10	0.891	11232384.9	91.2
4	Betaine	$C_5 H_{11} N O_2$	117.07	0.878	103358308.2	91.1
5	Choline	$C_5 H_{13} N O$	71.07	0.822	27689546.01	90.8
6	L-Norleucine	$C_6 H_{13} N O_2$	131.09	1.271	25798884.92	89.8
7	Curcumin	$C_{21} H_{20} O_6$	368.12	62.336	2506381.809	88.4
8	Psilostachyin B	$C_{15} H_{18} O_4$	230.1	1.439	8288454.35513165	87.5
9	Peruvinine	$C_{15} H_{20} O_4$	264.13	1.455	16685461.67	87.4
10	DL-Stachydrine	$C_7 H_{13} N O_2$	143.09	0.867	4057596.442	87.4
11	L-Aspartic acid	$C_4 H_7 N O_4$	133.03	0.759	1652585.893	86.8
12	2-Hydroxyphenylalanine	$C_9 H_{11} N O_3$	181.07	1.264	4438698.375	86.7
13	Pipecolic acid	$C_6 H_{11} N O_2$	129.07	1.252	8121221.514	86.4
14	Indole-3-acrylic acid	$C_{11} H_9 N O_2$	187.06	1.289	2735172.522	85.5
15	(-)-Caryophyllene oxide	$C_{15} H_{24} O$	220.18	62.066	1462034.826	85.2
16	Antheindurolide A	$C_{15} H_{20} O_4$	264.13	37.085	425711.3299	85.1

modifications or specialized delivery systems to enhance their bioavailability.

3.2. Molecular docking analysis

Molecular docking results against PD-L1 and CTLA-4 showed varied binding potentials among the analyzed compounds based on their binding energy values (Table 3). These results can serve as a basis for understanding the potential activity of bioactive compounds in inhibiting both key targets in immunology-based cancer therapy. Based on binding energy values, Psilostachyin B exhibited the highest affinity for PD-L1 and CTLA-4, with binding energy values of −6.9 and −6.8 kcal/mol, respectively. These values indicate stronger binding compared to the native ligand and the drug control (Doxorubicin). Additionally, doxorubicin also demonstrated strong binding affinity, with binding energy values of −6.1 kcal/mol and −6.7 kcal/mol for PD-L1 and CTLA-4, respectively. In contrast, choline-like compounds exhibited the weakest binding affinity, with binding energy values of −2.9 kcal/mol for PD-L1 and -3.2 kcal/mol for CTLA-4. Overall, compounds from the combination of *C. longa* and *P. niruri* demonstrate potential as inhibitors of PD-L1 and CTLA-4, making them promising candidates for cancer treatment. Molecular docking is a computational approach used to predict interactions between small molecules (ligands) and protein targets, especially in the development of immune checkpoint inhibitors for cancer therapy [35]. Immune checkpoints, such as PD-1, PD-L1, and CTLA-4, play a crucial role in regulating the immune system and are often exploited by cancer cells to evade immune responses. Molecular docking studies of immune checkpoint inhibitors aim to assess the potential binding affinity of a compound to a target protein, thereby assisting in the design and development of more effective drugs [36]. Based on the molecular docking results, Psilostachyin B was identified as the most promising compound among the tested ligands. Subsequently, its interactions with key residues of CTLA-4 and PD-L1 were further analyzed.

Molecular docking analysis showed that the inhibitor and Doxorubicin exhibit significant similarities in interacting with key PD-L1 residues, namely TYR32, SER80, ARG84, ASP103, GLN107, LEU106, LYS105, HIS140, and GLU139. The inhibitor formed hydrophobic, hydrogen bonding, and van der Waals interactions with almost all of these key residues, indicating high affinity and specificity toward the PD-L1 active site. Doxorubicin exhibited hydrophobic interactions with ARG84 and hydrogen bonds with SER79 and SER80, while its van der Waals interactions involved TYR32, ASP103, LYS105, GLN107, GLU139, and HIS140. Meanwhile, Psilostachyin B exhibited hydrophobic interactions with ILE65, LEU74, ARG86, and LEU89. It also formed a hydrogen bond with GLN77. In addition, its van der Waals interactions involved several residues, including ILE64, GLN66, PHE67, GLU72, ASP73, GLN83, ALA85, and LYS89 (Fig. 2b). The interactions between a ligand and a protein—such as hydrogen bonds, hydrophobic interactions, and van der Waals forces—are essential for determining binding affinity and complex stability. Hydrogen

Table 3. Molecular docking results of C. longa *and* P. niruri *bioactive compounds.*

No	Name	Pubchem ID	Binding Energy (kcal/mol)	
			PD-L1	CTLA-4
1	Trigonelline	5570	−4.1	−4.3
2	Erucamide	5365371	−4	−4.2
3	DL-Carnitine	288	−3.7	−3.9
4	Betaine	247	−3.2	−3.2
5	Choline	305	−2.9	−3.2
6	L-Norleucine	21236	−3.8	−4
7	Curcumin	969516	−6	−6.6
8	Psilostachyin B	5320768	−6.9	−6.8
9	Peruvinine	75368817	−5.9	−6.7
10	DL-Stachydrine	555	−4	−4.3
11	L-Aspartic acid	5960	−4.2	−4.1
12	2-Hydroxyphenylalanine	91482	−4.5	−5.2
13	Pipecolic acid	849	−3.9	−4.5
14	Indole-3-acrylic acid	5375048	−5.2	−5.8
15	(-)-Caryophyllene oxide	1742210	−5.3	−5.7
16	Antheindurolide A	14733728	−5.8	−6.1
17	Inhibitor	117951478/24139	−5.7	−5.6
18	Doxorubicin	31703	−6.1	−6.7

bonds are among the most common and significant motifs in biological systems, contributing to both binding affinity and selectivity [37].

The results of molecular docking against CTLA-4 protein showed that the three ligands, namely native ligand, doxorubicin, and Psilostachyin B interacted with a number of residues previously predicted as part of the active site, namely VAL104, GLU77, PRO74, PHE134, PRO135, ASP107, LYS105, LEU189, and ALA106. The native ligand showed van der Waals interactions with almost all key residues and formed two hydrogen bonds with residues VAL104 and ALA106. Doxorubicin interacted with most of the key residues by forming three hydrogen bonds, at residues GLU77 and ALA106, and a hydrophobic interaction at LEU189. Psilostachyin B did not show hydrogen bond formation but showed a predominance of strong hydrophobic interactions with key residues such as PRO74, VAL104, ALA106, and PHE134. These interactions show good binding potential although through different mechanisms. The interaction of Psilostachyin B with some of the same key residues as the inhibitor and Doxorubicin suggests that Psilostachyin B has potential as a CTLA-4 ligand candidate (Fig. 1b). In this case, Psilostachyin B did not exhibit direct interactions with the predicted active site residues. Nevertheless, it formed a greater number of hydrophobic and van der Waals interactions, which can contribute to the overall stability of the complex. Hydrophobic interactions play a crucial role in maintaining long-term stability, especially within non-polar environments, while van der Waals forces, although weaker and less specific, help sustain surface contact between the ligand and the protein [38].

3.3. Molecular dynamics simulation

Molecular dynamics (MD) simulations have become a crucial tool in understanding the behavior and stability of molecular systems, especially in the context of drug design and protein-ligand interactions [39]. In immunotherapy development, MD simulation plays a crucial role in evaluating the

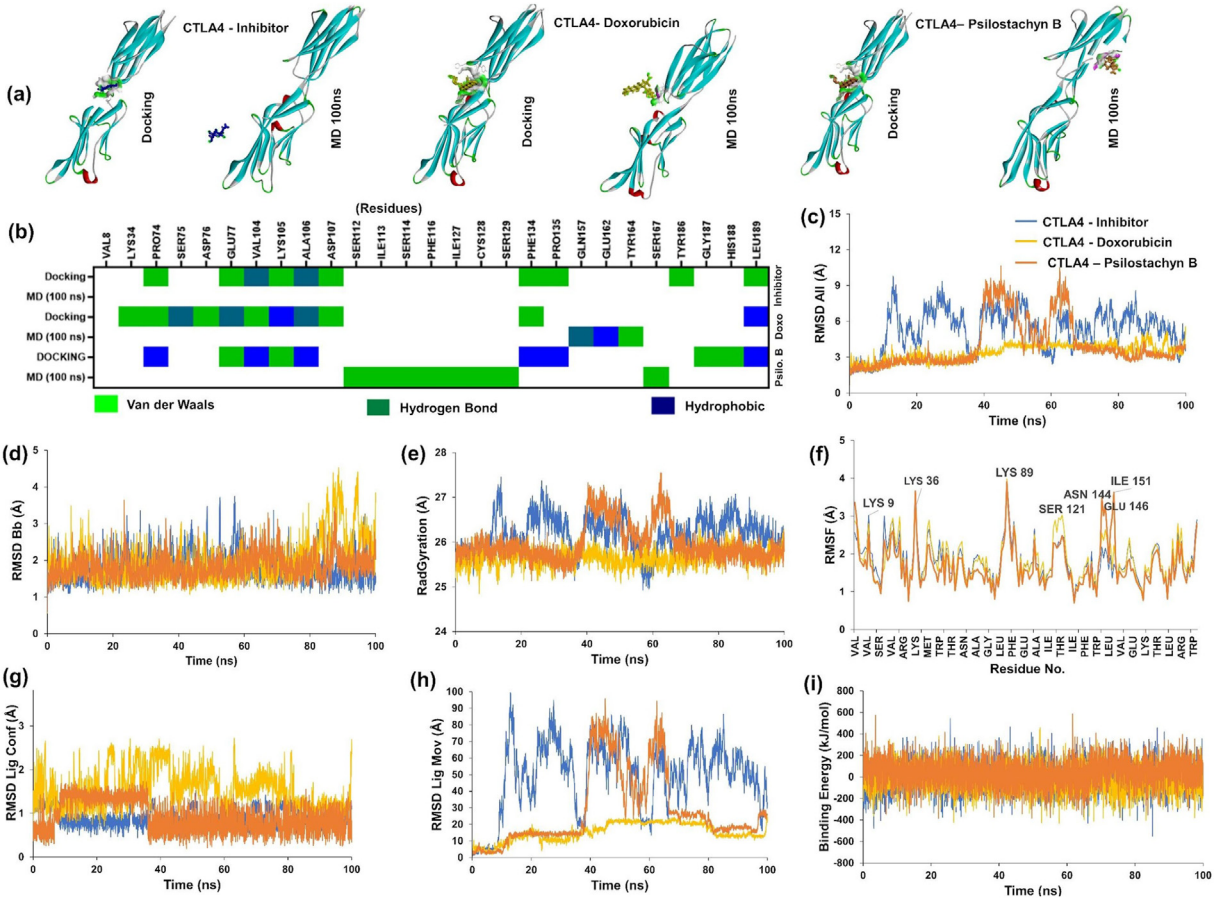

Fig. 1. Molecular docking and molecular dynamics simulation of the potential compound with CTLA-4. a). CTLA-4 visualization Molecular docking and dynamics simulation of potential compound, b). Residues interaction of potential compound, c) RMSD All (complex-ligand) Simulation, d). RMSD Backbone (Bb) simulation, e) Radius gyration simulation, f) RMSF simulation, g) RMSD ligand conformation simulation, h) RMSD ligand movement simulation, i) Number of hydrogen bond j) MM/PBSA Binding energy simulation.

stability of the interaction between a ligand and its target protein in a physiological environment. By simulating changes in molecular structure on a unit time scale, this method provides valuable insights into the binding mechanism, conformational dynamics, and stability of protein-ligand complexes, thus laying the foundation for the development of more effective immune therapies [40]. In this study, MD simulations were employed to evaluate the stability, binding affinity, and conformational behavior of Psilostachyin B in its interactions with CTLA-4 and PD-L1 proteins. The results from MD simulations provide valuable insights into the dynamic properties of Psilostachyin B-protein complexes, which cannot be fully elucidated through static docking studies alone. Notably, MD simulations revealed that Psilostachyin B exhibited a more stable binding interaction compared to the native ligand. These findings suggest that Psilostachyin B maintains a more stable conformation throughout the simulations, highlighting its potential as a promising immune checkpoint inhibitor candidate for cancer therapy.

Binding site molecular docking and molecular dynamics simulation showed that different residues exhibited distinct flexibility and interaction profiles, influencing the overall ligand binding conformation. The results of molecular docking and molecular dynamics (MD) simulations demonstrated that the Psilostachyin B has potential to be used as an agent that interacts with CTLA-4. In Fig. 1a, visualization of the molecular docking and MD simulation results revealed that the native ligand detached from the active site and lost its interaction with the CTLA-4 protein, indicating instability in binding to the target. In contrast, both Doxorubicin and Psilostachyin B exhibited changes in ligand interaction throughout the 100 ns MD simulation, suggesting dynamic binding to the CTLA-4 protein. Fig. 1b illustrates the changes in residue interactions between molecular docking and MD simulation results. In the docking analysis, residues Glu77, Val104, Lys105, Ala106, and Phe134 acted as the primary interaction sites. On the other hand, the interaction of the inhibitor with CTLA-4 shows an unstable interaction as shown by the final results of the simulation, that the inhibitor ligand is separated from the protein complex. This result is supported by the results of the Ligand Movement inhibitor analysis which shows fluctuations after 10 ns. This could be due to the influence of temperature and water content during the simulation. Meanwhile, Psilostachyin B and doxorubicin showed interaction during the 100 ns simulation with differences in the interaction results with the docking results (Fig. 1b). However, during the MD simulation, the ligand interaction pattern changed, suggesting that the ligand-protein complex undergoes structural adaptation, which may influence the stability and effectiveness of the binding. The CTLA-4–Psilostachyin B complex exhibited a stable RMSD value during the initial 40 ns of the simulation and regained stability after 80 ns, with an RMSD value below 3 Å (Fig. 1c). In comparison, the CTLA-4-inhibitor complex initially maintained a stable bond during the first 10 ns but exhibited fluctuating ligand-protein interactions throughout the remainder of the simulation, with RMSD values reaching 6–9 Å. Meanwhile, the drug control Doxorubicin demonstrated a more stable complex at 50 ns, with an RMSD value below 3 Å. Interestingly, Psilostachyin B followed a similar trend of Doxorubicin after 70 ns, indicating its potential to maintain a stable interaction with CTLA-4.

The backbone RMSD values of the three complexes remained within the range of 1–3.5 Å, indicating that the backbone structure remained relatively stable throughout the simulation (Fig. 1d). Among the three, the CTLA-4–Doxorubicin complex exhibited the least fluctuation, suggesting that its interaction with Doxorubicin helped maintain the backbone structure more effectively. RMSD (Root Mean Square Deviation) Backbone (Bb) is a specific metric used to evaluate the stability of the main skeleton or compact structure of proteins. It is particularly useful in assessing the structural stability and conformational changes of proteins during simulations or experimental studies [41]. Meanwhile, the CTLA-4–Inhibitor complex showed higher fluctuations but remained within an acceptable range. Furthermore, the Radius of Gyration (Rg) measures the degree of density or compactness of the protein structure during the simulation. A lower Rg value indicates a more compact structure. The CTLA-4–Inhibitor complex exhibited significant fluctuations between 25 and 27.5 Å, suggesting a more extended protein structure. Similarly, the CTLA-4–Psilostachyin B complex followed a comparable trend but displayed slightly greater stability. In contrast, the CTLA-4–Doxorubicin complex had the lowest Rg value, stabilizing around 25–26 Å, indicating that its interaction with Doxorubicin maintained a more compact protein structure (Fig. 1e). Root Mean Square Fluctuation (RMSF) analysis, as shown in Fig. 2f, revealed that the CTLA-4–Inhibitor complex experienced instability at Lys9, Lys36, and Lys89. Meanwhile, Doxorubicin exhibited fluctuations at Ser121, and Psilostachyin B showed instability at Lys36, Lys89, Asn144, Glu146, and Ile151.

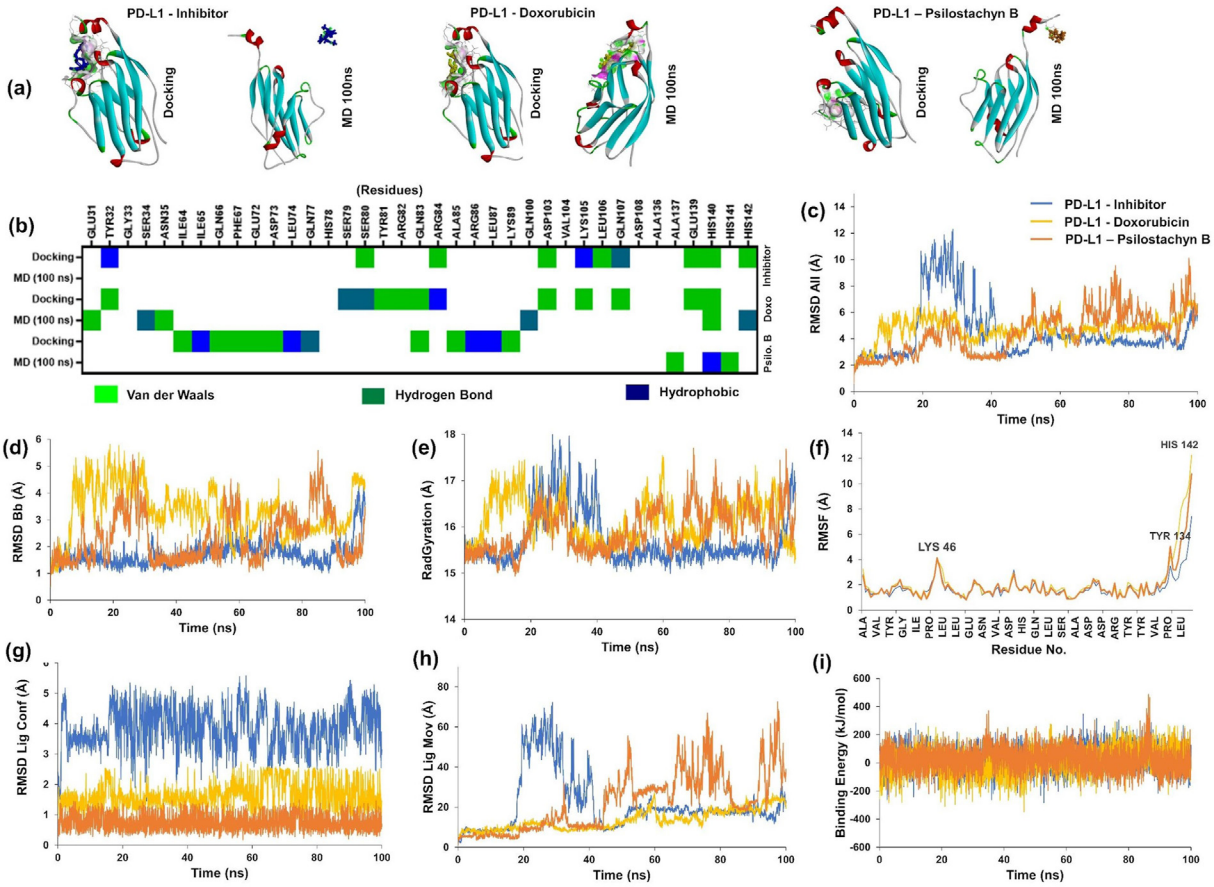

Fig. 2. Molecular docking and molecular dynamics simulation of potential compound with PD-L1. a). PD-L1 visualization molecular docking and dynamics simulation of potential compound, b). Residues interaction of potential compound, c) RMSD All (complex-ligand) Simulation, d). RMSD Backbone (Bb) simulation, e) Radius gyration simulation, f) RMSF simulation, g) RMSD ligand conformation simulation, h) RMSD ligand movement simulation, i) Number of Hydrogen Bond j) MM/PBSA Binding energy simulation.

The RMSD Ligand Conformation analysis shows that the CTLA-4–Inhibitor complex exhibited the most stable RMSD throughout the 100 ns simulation, with an RMSD value of approximately 1–3 Å, indicating that the ligand remained stable (Fig. 1g). RMSD Ligand Conformation is used to assess the conformational changes of the ligand during simulation, reflecting its structural flexibility [42]. In contrast, the RMSD Ligand Movement analysis reveals that the CTLA-4–Inhibitor complex fluctuated after 10 ns, while the CTLA-4–Psilostachyin B complex began fluctuating after 40 ns. Meanwhile, the CTLA-4–Doxorubicin complex demonstrated better ligand stability over the entire 100 ns simulation (Fig. 1h). As an immune checkpoint inhibitor drug candidate, maintaining protein-ligand interactions for at least 10 ns is sufficient to exert a CTLA-4 inhibitory effect, as observed with the native ligand. On the other hand, CTLA-4-Doxorubicin showed the best number of hydrogen bonds from the beginning to the end of the simulation, while CTLA-4- Psilostachyin B showed hydrogen bonds from the beginning of the simulation up to 38 ns and again formed hydrogen bonds at 80 ns until the end of the simulation, while CTLA-4-inhibitor showed hydrogen bond loss after 10 ns (Fig. 1i). Therefore, CTLA-4–Psilostachyin B has the potential to be an effective CTLA-4 inhibitor drug candidate, as it exhibits stronger protein-ligand interaction potential compared to the native ligand and performs similarly to the drug control. This conclusion is further supported by the binding energy values based on MM/PBSA method, which indicate the interaction energy between the protein and ligand during the simulation. The CTLA-4–Psilostachyin B complex showed a positive value of 37.713 kJ/mol and exhibited more stable binding energy values compared to both the inhibitor and Doxorubicin, with average values of −6.951 kJ/mol and −20.845 kJ/mol, respectively, reinforcing its potential as a novel inhibitor targeting CTLA-4.

CTLA-4 as a negative immune checkpoint plays a crucial role in regulating T cell activation and maintaining immune system homeostasis [43]. In

the context of cancer, high CTLA-4 expression contributes to the suppression of effector T cell (Teff) activation and proliferation, while increasing the activity of immunosuppressive regulatory T cells (Treg) [44]. Inhibition of CTLA-4 disrupts its interaction with CD80/CD86, which are found on antigen-presenting cells (APCs). This mechanism promotes enhanced activation of CD8+ T cells while reducing Treg dominance in the TME, ultimately strengthening the antitumor immune response [45]. Furthermore, by decreasing the Treg/Teff ratio through CTLA-4 inhibitors in the tumor environment, this approach has the potential to increase cytotoxicity against cancer cells and improve the effectiveness of immune-based cancer therapies. Therefore, CTLA-4 inhibition is one of the primary strategies in cancer immunotherapy development to enhance antitumor immune responses.

Interaction analysis of the PD-L1 protein with various ligands was performed using molecular docking and molecular dynamics (MD) simulations over 100 ns. Binding site molecular dynamics (MD) simulations revealed the involvement of different residues compared to the molecular docking results, potentially influencing the overall ligand binding conformation. The simulation results revealed that the native ligand experienced detachment from the active site, indicating an unstable interaction with PD-L1. In contrast, Doxorubicin and Psilostachyin B exhibited sustained interactions throughout the simulation, suggesting that these two compounds have the potential to act as more effective PD-L1 inhibitors compared to the native ligand. However, Psilostachyin B maintained interactions with several residues—ALA137, HIS140, and HIS141—after 100 ns of simulation. The residual interaction analysis (Fig. 2b) indicates that at the molecular docking stage, the interaction profiles were diverse. However, during the 100 ns MD simulation, the interaction pattern shifted, demonstrating dynamic adjustments in ligand binding with the PD-L1 protein, with His140 identified as a key residue. In contrast, the inhibitor lost its interactions with PD-L1 residues during the 100 ns simulation, indicating instability in the ligand–protein interaction (Fig. 2b). Furthermore, molecular dynamics simulation results confirmed that Psilostachyin B and Doxorubicin maintained crucial interactions with PD-L1, whereas the native ligand/inhibitor exhibited loss of binding with the protein complex.

The stability of the ligand-protein complex was analyzed through RMSD All, which showed that the native ligand/inhibitor experienced high fluctuation after 20 ns, indicating instability in its interaction with PD-L1. In contrast, Doxorubicin exhibited fluctuation after 10 ns. Psilostachyin B demonstrated a more stable RMSD pattern compared to both the inhibitor and the control drug (Fig. 2c). The backbone RMSD (RMSD Bb) values for the three complexes showed distinct fluctuation patterns during the simulation. The PD-L1–inhibitor complex maintained relatively stable RMSD values below 3 Å, indicating stable binding conformation, whereas the PD-L1–Doxorubicin and PD-L1–Psilostachyin B complexes exhibited higher fluctuations, with RMSD values approaching 6 Å. These results suggest that the inhibitor complex is more structurally stable compared to the other two complexes (Fig. 2d). However, the PD-L1-Doxorubicin complex exhibited an RMSD Bb value exceeding 3 Å after 10 ns, which persisted until the end of the simulation, indicating a conformational change in the protein structure. This observation is further supported by the Radius of Gyration (Rg) values, where the PD-L1-Doxorubicin complex displayed continuous fluctuations from the start of the simulation. Radius of Gyration (Rg) is used to evaluate the compactness of the protein structure during simulation (Fig. 2e). A stable Rg value indicates that the protein-ligand complex maintains its structural shape well, which may indicate the stability of the ligand interaction with the target protein [46]. In contrast, the PD-L1-Psilostachyin B complex exhibited Rg values similar to those of the native ligand/inhibitor, suggesting that the PD-L1 complex remained more compact, and its protein structure was more stable compared to that of Doxorubicin.

Root Mean Square Fluctuation (RMSF) analysis (Fig. 2f) indicates that certain residues, particularly LYS 46, TYR 134, and HIS 142, exhibit high fluctuations, which may affect the flexibility of the active site and the effectiveness of ligand binding. The RMSD of Ligand Conformation reveals that the PD-L1-inhibitor complex maintained an RMSD above 3 Å throughout the 100 ns simulation, suggesting that the ligand conformation was unstable. It has been reported that RMSF provides information regarding the flexibility of protein residues, where high RMSF values at certain residues may indicate regions that are more flexible or more prone to conformational changes [47]. In contrast, Doxorubicin and Psilostachyin B in complexes with PD-L1 exhibited RMSD values below 3 Å, indicating greater structural stability (Fig. 2g). Meanwhile, the RMSD of Ligand Movement analysis shows that the PD-L1-inhibitor complex experienced fluctuations after 20 ns. Compared to this finding, Psilostachyin B maintained lower RMSD values up to 20 ns before exhibiting greater fluctuations after 40 ns. The PD-L1-Doxorubicin complex demonstrated better

ligand stability over the 100 ns simulation period (Fig. 3h). RMSD Ligand Movement shows the dynamics of ligand movement within the active site of the protein. If the RMSD of the ligand remains stable within the simulation time span, it indicates a strong and specific interaction between the ligand and the target protein [48,49]. The number of hydrogen bonds formed between PD-L1 and Psilostachyin B was higher than that of the inhibitor during the first 40 ns of simulation and was relatively similar to the number observed with both the inhibitor and Doxorubicin after 40 ns. The presence of hydrogen bonds throughout the simulation potentially supports stable interactions between the ligands and PD-L1 (Fig. 2i).

The binding energy analysis further supports these findings, as the PD-L1–Psilostachyin B complex exhibited relatively stable binding energy values throughout the simulation. This suggests strong interactions with PD-L1, as indicated by the MM/PBSA method analysis (Fig. 2j). All average binding energy values from the MM/PBSA analysis for Doxorubicin, Psilostachyin B, and the inhibitor were positive binding, with values of 7.632 kJ/mol, 28.053 kJ/mol, and 29.683 kJ/mol, respectively. These results indicate that Psilostachyin B has the potential to act as a novel PD-L1 inhibitor, as its binding energy closely approaches that of the native inhibitor. This interaction may contribute to PD-L1 inhibition within the TME, potentially enhancing the immune response against cancer cells.

PD-L1 is a key protein at immune checkpoint sites that enables cancer cells to evade immune surveillance by binding to PD-1 on T cells, thereby suppressing T cell activity and promoting cancer progression [50]. PD-L1 is frequently upregulated in various cancers, often in response to inflammatory signals such as IFN-γ, and its expression is associated with poor prognosis due to its role in immune suppression [51]. In immunotherapy, PD-L1 is targeted by immune checkpoint inhibitors (ICIs), such as anti-PD-1/PD-L1 antibodies, which have shown the potential to restore immune system function by modulating T cell activity and have demonstrated

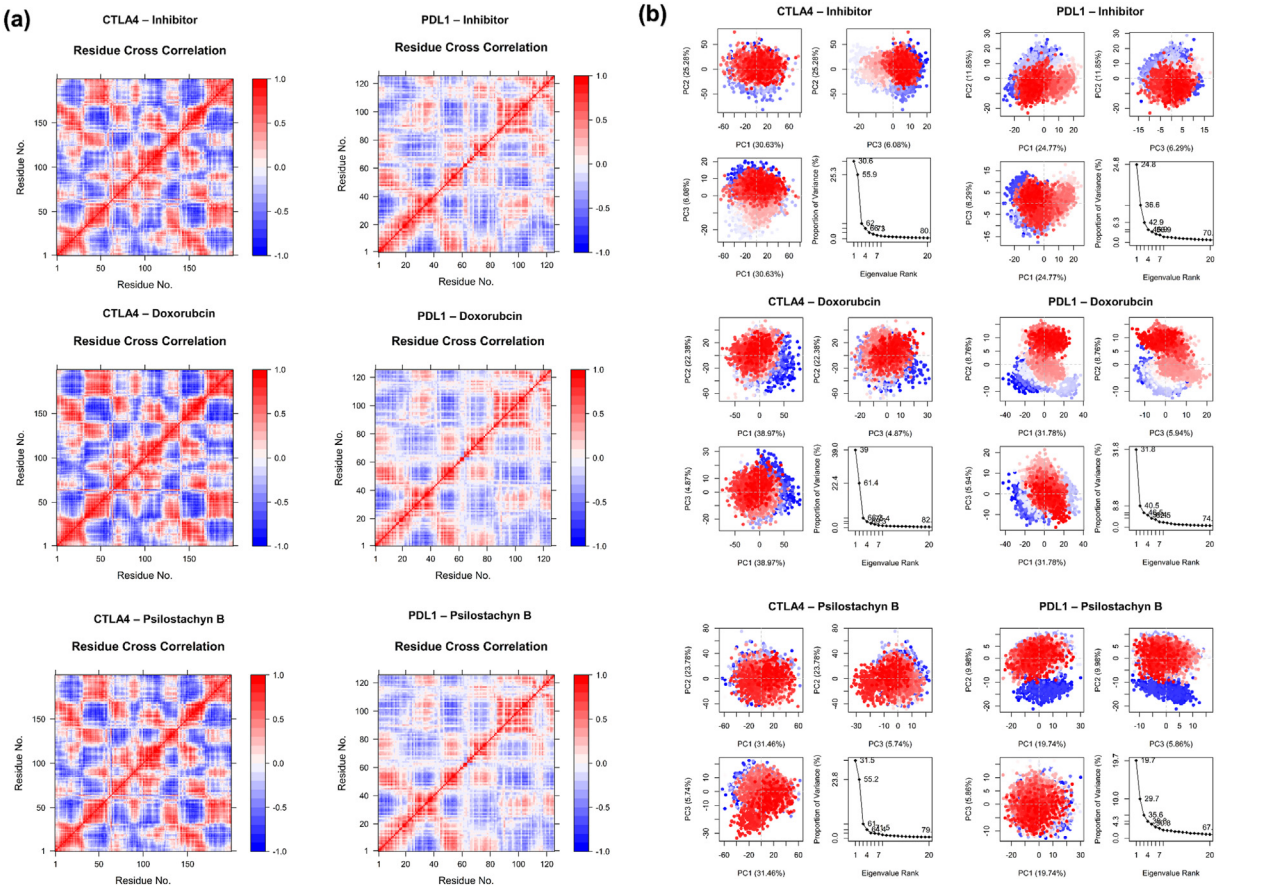

Fig. 3. Dynamic Cross-Correlation Matrix (DCCM) and Principal Component Analysis (PCA) during 100 ns Molecular Dynamics Simulations. (a) DCCM analysis illustrating the correlated motions of Cα atoms throughout the simulation. Red indicates a positive correlation (parallel motion), and blue indicates a negative correlation (antiparallel motion). (b) PCA shows conformational changes over time, with a color gradient from blue (initial frame) to red (final frame), representing the progression of structural dynamics.

significant clinical efficacy. Moreover, PD-L1 expression serves as a predictive biomarker for response to immunotherapy; however, resistance mechanisms—such as the activation of alternative immune checkpoints and impaired antigen presentation—pose significant challenges to treatment efficacy [52]. Therefore, targeting PD-L1 in cancer therapy offers a promising opportunity to restore immune system function in patients.

Dynamic Cross-Correlation Matrix (DCCM) and Principal Component Analysis (PCA) analyses were employed to evaluate the dynamics and conformational stability of CTLA-4 and PD-L1 protein complexes over 100 ns molecular dynamics simulations at 310 K. The Dynamic Cross-Correlation Matrix (DCCM) analysis of Cα atoms also revealed that the CTLA-4 and PD-L1 complex favored parallel conformational movements over antiparallel ones. The molecular interaction of CTLA-4–Psilostachyn B and PD-L1–Psilostachyn B tends to compact the protein conformation, consistent with the observed stability and interaction strength of the complex, as indicated by red-colored regions with correlation values close to +1. These patterns reflect synchronized movement in the same direction, suggesting a more coherent and stable dynamic behavior [53]. The broader presence of parallel correlations and the reduction of antiparallel motions in the Psilostachyn B complex further underscore its potential as a ligand capable of enhancing the structural stability of CTLA-4 and PD-L1 more effectively than the controls (Fig. 3a). The interactions involving Glu77, Val104, and Ala106 play a critical role in maintaining the stability of the Psilostachyn B–CTLA-4 complex. These residues exhibit prominent interactions with Psilostachyn B, supported by increased non-bonded contacts that further enhance the overall stability of the complex. However, LYS46, TYR134, and HIS142 show non-stable interactions, while HIS140 plays a critical role in maintaining the stability of the Psilostachyn B–CTLA-4 complex. The involvement of these key residues is likely crucial for preserving the structural integrity and ligand recognition of CTLA-4 and PD-L1, particularly in the context of its role in immune modulation.

Principal Component Analysis (PCA) analyses were employed to evaluate the dynamics and conformational stability of CTLA-4 and PD-L1 protein complexes during 100 ns molecular dynamics simulations at the physiological temperature of 310 K. PCA was used to reduce the complexity of the trajectory data and to identify the dominant collective modes of motion within the system. The resulting eigenvalues represent the amount of variance explained by each principal component. The CTLA-4 complexes with the native inhibitor and Doxorubicin exhibited cumulative PC1 and PC2 values of 55.9 % and 61.4 %, respectively, indicating dominant conformational fluctuations and potential instability under physiological conditions. In contrast, the complex with Psilostachyn B demonstrated a slightly lower cumulative variance of 55.2 %, suggesting a more evenly distributed and stable conformational motion throughout the simulation (Fig. 3b). These results were further supported by Root Mean Square Deviation (RMSD) and Root Mean Square Fluctuation (RMSF) analyses, in which all complexes showed values below 3 Å, indicating minimal structural fluctuations and favorable conformational stability. Furthermore, PCA revealed that the cumulative PC1 and PC2 values for the PD-L1 complexes with the reference inhibitor, Doxorubicin, and Psilostachyn B were 36.6 %, 40.5 %, and 29.7 %, respectively (Fig. 3b). The lower cumulative value observed in the PD-L1–Psilostachyn B complex indicates reduced conformational motion and suggests enhanced structural stability. This finding is further corroborated by RMSD analysis, which demonstrated that the PD-L1–Psilostachyn B complex exhibited lower structural fluctuations compared to the control. Collectively, these results suggest that Psilostachyn B may effectively stabilize PD-L1, highlighting its potential as a novel immune checkpoint inhibitor candidate through modulation of PD-L1 dynamics.

Psilostachyin B compounds exhibit potential as therapeutic agents targeting key proteins involved in immune response mechanisms and cancer progression. Mass spectrometry results showed the analysis of Psilostachyin B compound with a RT value of 1.439 min. The mass spectrum displays several peaks with the main ion at m/z 231.10046 [M+H]+, which indicates the presence of the target compound in protonated form. In addition, a methanol adduct ion was observed at m/z 263.12643 [M + H + MeOH]+ (Fig. 4a), and the 2D structure of compound Psilostachyin B is shown in Fig. 4b. Protein interaction analysis (Fig. 4c) revealed that Psilostachyin B interacts with several important proteins, including the molecular docking targets CTLA-4 and PD-L1, although indirectly. These interactions suggest that this compound may participate in regulating various molecular pathways implicated in cancer pathogenesis and TME dynamics. Furthermore, Gene Ontology (GO) analysis (Fig. 4d) demonstrated that Psilostachyin B exhibits immunosuppressive potential through multiple biological mechanisms associated with inflammatory response and immunomodulation, especially via the regulation of inflammatory response,

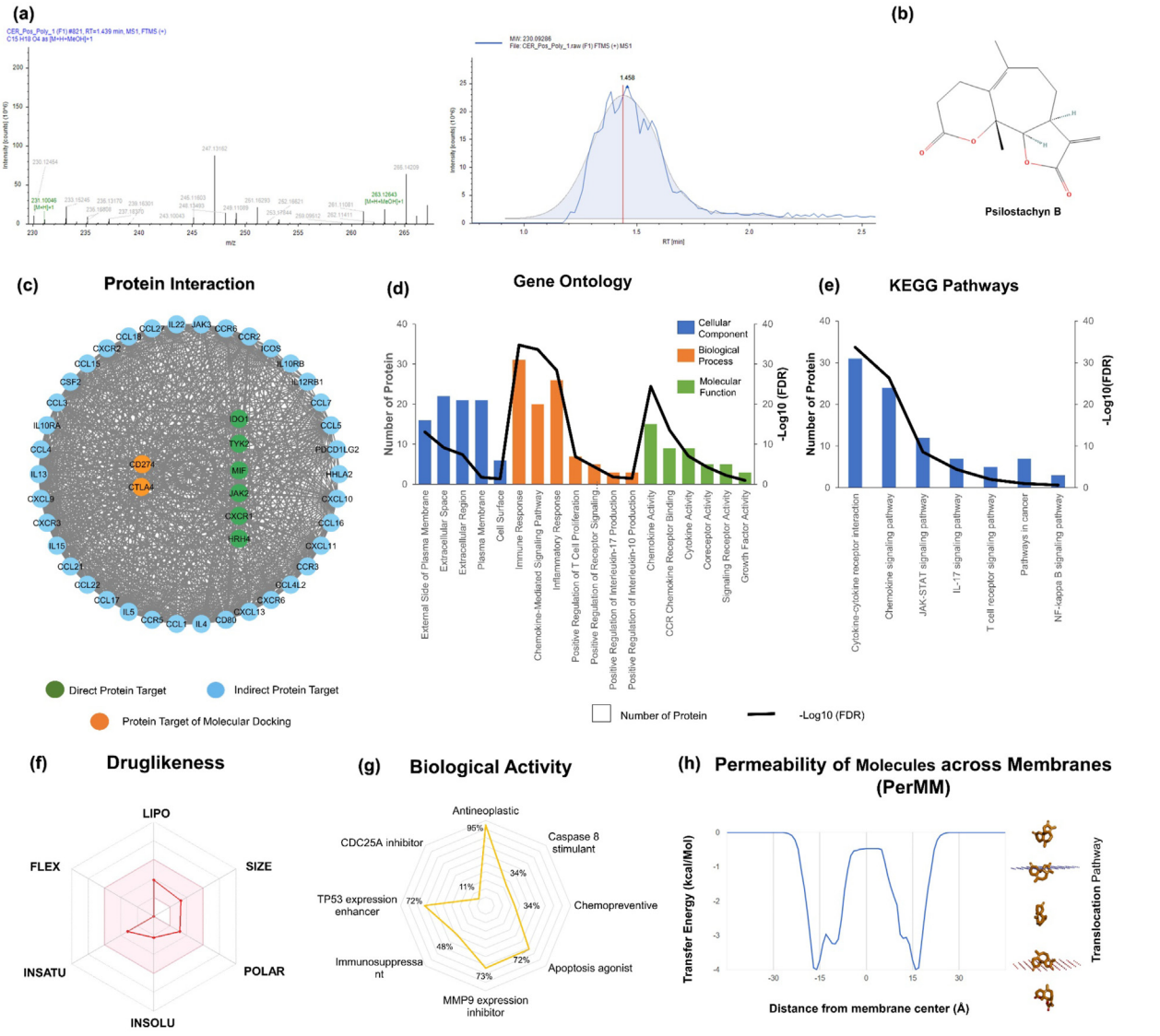

Fig. 4. Protein network and potential activity of Psilostachyn B. a) Single chromatogram of Psilostachyn B, b) 2D structure of Psilostachyn B, c) Protein–Protein Interaction Network, d) Gene Ontology, e) functional annotation based on database KEGG pathway, f) Drug-likeness on SWISS Adme Prediction, g) Probability of biological activity, and h) PerMM of Psilostachyn B.

immune system activation, and T-cell proliferation. This highlights the role of Psilostachyin B in modulating the TME, a critical factor in cancer development and progression. These findings are further supported by the KEGG pathway analysis (Fig. 4e), which indicates that Psilostachyin B significantly influences inflammatory responses and chemokine pathways. These pathways are known to be pivotal in immune cell infiltration, cellular communication within the tumor environment, and cancer metastasis regulation.

Moreover, Psilostachyin B demonstrates significant potential as a drug candidate based on its drug-likeness assessment. The compound exhibits a well-balanced profile of lipophilicity, polarity, and molecular flexibility, which facilitates efficient absorption and distribution within the body (Fig. 4f). Prediction results of potential biological activities (Fig. 4g) indicate that Psilostachyin B has a high probability of activity (Pa) as an antineoplastic agent (95 %), as well as a Caspase 8 stimulant, TP53 expression inducer, immunosuppressant agent, apoptosis agonist, Chemopreventive, MMP9 expression inhibitor, and CDC25A inhibitor. These activities suggest that Psilostachyin B may suppress tumor growth by inducing apoptosis and inhibiting cancer cell proliferation while modulating immune components within the tumor microenvironment. Furthermore, energy transfer analysis using the PerMM method (Fig. 4h) reveals that the free

energy of binding between Psilostachyin B and the DOPC membrane is −4.01 kcal/mol at pH 7 and 310K, indicating a stable molecular interaction with the cell membrane environment. This stability could play a crucial role in the uptake and distribution of the compound within biological systems, thereby supporting its potential as an anticancer drug candidate.

4. Conclusion

Immunotherapy-based treatment is considered an effective strategy for modulating the TME. This study explores the potential of immunotherapy by utilizing molecular docking and molecular dynamics simulations to evaluate bioactive compounds from *Curcuma longa* and *Phyllanthus niruri* as immune checkpoint inhibitor candidates targeting CTLA-4 and PD-L1. The findings of this study indicate that Psilostachyin B emerges as the most promising candidate among the compounds identified in *C. longa* and *P. niruri*. Molecular dynamics simulations indicated that Psilostachyin B had greater stability than both the positive control and known inhibitors, as supported by favorable RMSD, radius of gyration, and RMSF values. MM/PBSA analysis also demonstrated strong binding affinity, with negative binding free energy values, indicating thermodynamically favorable complex formation. In addition, DCCM analysis revealed correlated motions within the binding region, and Principal Component Analysis (PCA) showed limited conformational shifts, further supporting the stability of Psilostachyin B during the simulation. These findings suggest that natural products derived from *C. longa* and *P. niruri*, such as Psilostachyin B, have the potential to modulate the TME, thereby enhancing immune responses against cancer cells. The molecular dynamics promised that Psilostachyin B is a molecule which has superior stability compared native ligands, as evidenced by favorable RMSD values. Additionally, Psilostachyin B targets multiple key proteins involved in immunosuppressive mechanisms, especially through chemokine, cytokine, and JAK-STAT signaling pathways, exhibiting strong biological activity scores. However, further validation through comprehensive studies is necessary. For future research, extending computational simulations to include variations in temperature and longer simulation times is recommended. Additionally, validation through in vitro and in vivo studies remains essential to confirm the efficacy and safety of Psilostachyin B in the development of cancer immunotherapy.

Ethics information

None.

Funding

None.

Conflicts of interest

All the authors declare that there are no conflicts of interest.

Acknowledgements

The authors would like to provide their appreciation for the facilities support from Laboratorium Riset Terpadu - Universitas Brawijaya (LRT-UB).

References

[1] X. Li, Y. Guo, M. Xiao, W. Zhang, The immune escape mechanism of nasopharyngeal carcinoma, FASEB J 37 (2023) 1–20, https://doi.org/10.1096/fj.202201628RR.
[2] M.T. Bilotta, A. Antignani, D.J. Fitzgerald, Managing the TME to improve the efficacy of cancer therapy, Front. Immunol. 13 (2022) 1–10, https://doi.org/10.3389/fimmu.2022.954992.
[3] S. Gaikwad, M.Y. Agrawal, I. Kaushik, S. Ramachandran, S.K. Srivastava, Immune checkpoint proteins: signaling mechanisms and molecular interactions in cancer immunotherapy, Semin. Cancer Biol. 86 (2022) 137–150, https://doi.org/10.1016/j.semcancer.2022.03.014.
[4] H. Zhang, Z. Dai, W. Wu, Z. Wang, N. Zhang, L. Zhang, W.-J. Zeng, Z. Liu, Q. Cheng, Regulatory mechanisms of immune checkpoints PD-L1 and CTLA-4 in cancer, J. Exp. Clin. Cancer Res. 40 (2021) 1–22, https://doi.org/10.1186/s13046-021-01987-7.
[5] F. Shan, A. Somasundaram, T.C. Bruno, C.J. Workman, D.A.A. Vignali, Therapeutic targeting of regulatory T cells in cancer, Trends Cancer 8 (2022) 944–961, https://doi.org/10.1016/j.trecan.2022.06.008.
[6] X. Zhou, Y. Ni, X. Liang, Y. Lin, B. An, X. He, X. Zhao, Mechanisms of tumor resistance to immune checkpoint blockade and combination strategies to overcome resistance, Front. Immunol. 13 (2022) 1–25, https://doi.org/10.3389/fimmu.2022.915094.
[7] M.K. Islam, J. Stanslas, Peptide-based and small molecule PD-1 and PD-L1 pharmacological modulators in the treatment of cancer, Pharmacol. Ther. 227 (2021) 1–21, https://doi.org/10.1016/j.pharmthera.2021.107870.
[8] E.N. Scott, A.M. Gocher, C.J. Workman, D.A.A. Vignali, Regulatory T cells: barriers of immune infiltration into the tumor microenvironment, Front. Immunol. 12 (2021) 1–10, https://doi.org/10.3389/fimmu.2021.702726.
[9] M. Haist, H. Stege, S. Grabbe, M. Bros, The functional crosstalk between myeloid-derived suppressor cells and regulatory T cells within the immunosuppressive tumor microenvironment, Cancers 13 (2021) 1–34, https://doi.org/10.3390/cancers13020210.
[10] L.J. Ajutor, B.A. Iyoyojie, K.U. Ugoagwu, O.T. Samuel, O.A. Adedayo, D.T. Oyedemi, D.E. Obasi, A.A. Christopher, A.P. Bemigho, C.A. Adobor, Role of immune checkpoints (PD-1, PDL1 and CTLA-4) in triple-negative breast cancer and therapeutic implications, Int. Res. J. Oncol. 8 (2025) 8–20, https://doi.org/10.9734/irjo/2025/v8i1170.
[11] Z.N. Willsmore, B.G.T. Coumbe, S. Crescioli, S. Reci, A. Gupta, R.J. Harris, A. Chenoweth, J. Chauhan, H.J. Bax,

A. McCraw, A. Cheung, G. Osborn, R.M. Hoffmann, M. Nakamura, R. Laddach, J.L.C. Geh, A. MacKenzie-Ross, C. Healy, S. Tsoka, J.F. Spicer, D.H. Josephs, S. Papa, K.E. Lacy, S.N. Karagiannis, Combined anti-PD-1 and anti-CTLA-4 checkpoint blockade: treatment of melanoma and immune mechanisms of action, Eur. J. Immunol. 51 (2021) 544–556, https://doi.org/10.1002/eji.202048747.

[12] V.E. Stefan, D.D. Weber, R. Lang, B. Kofler, Overcoming immunosuppression in cancer: how ketogenic diets boost immune checkpoint blockade, Cancer Immunol. Immunother. 74 (2024) 1–12, https://doi.org/10.1007/s00262-024-03867-3.

[13] P. Pandey, F. Khan, H.A. Qari, T.K. Upadhyay, A.F. Alkhateeb, M. Oves, Revolutionization in cancer therapeutics via targeting major immune checkpoints PD-1, PD-L1 and CTLA-4, Pharmaceuticals 15 (2022) 1–16, https://doi.org/10.3390/ph15030335.

[14] Y. Huang, Z. Chen, G. Shen, S. Fang, J. Zheng, Z. Chi, Y. Zhang, Y. Zou, Q. Gan, C. Liao, Y. Yao, J. Kong, X. Fan, Immune regulation and the tumor microenvironment in anti-PD-1/PDL-1 and anti-CTLA-4 therapies for cancer immune evasion: a bibliometric analysis, Hum. Vaccines Immunother. 20 (2024) 1–12, https://doi.org/10.1080/21645515.2024.2318815.

[15] F.N. Asyhari, H.S. Zulfatim, N.T.M. Putri, M. Dliyauddin, A.S. Jamil, A. Soewondo, M.H. Natsir, M. Ibrahim, S. Rahayu, M.S. Djati, M. Rifa'i, Expression of immunoglobulin M (IgM) and immunoglobulin G (IgG) in normal wistar rat post-cheral® administration, HAYATI J. Biosci. 31 (2024) 1030–1036, https://doi.org/10.4308/hjb.31.5.1030-1036.

[16] J. Ekowati, R. Widyowati, Norhayati, S.K. Jain, Chemopreventive practices in traditional medicine, in: S.C. Izah, M.C. Ogwu, M. Akram, eds., Herbal Medicine Phytochemistry, Springer International Publishing, Cham. 2023, pp. 1–54, https://doi.org/10.1007/978-3-031-21973-3_28-1.

[17] S. Fuloria, J. Mehta, A. Chandel, M. Sekar, N.N.I.M. Rani, M.Y. Begum, V. Subramaniyan, K. Chidambaram, L. Thangavelu, R. Nordin, Y.S. Wu, K.V. Sathasivam, P.T. Lum, D.U. Meenakshi, V. Kumarasamy, A.K. Azad, N.K. Fuloria, A comprehensive review on the therapeutic potential of *Curcuma longa* Linn. in relation to its major active constituent curcumin, Front. Pharmacol. 13 (2022) 1–27, https://doi.org/10.3389/fphar.2022.820806.

[18] W.E. Putra, A.M.L.S. Mentarõ, D. Ratnasarõ, D. Chaõrunnõza, A. Hidayatullah, M. Rifai, Immunosuppressive and ameliorative effects of dietary combined herbs extract of *Curcuma zedoaria* (Christm.) Roscoe and *Phyllanthus niruri* L. in DMBA-induced breast cancer mouse model, Fabad J. Pharm. Sci. 49 (2024) 91–110, https://doi.org/10.55262/fabadeczacilik.1329094.

[19] S.N.K. Rao G., R.R. Alavala, Applications of Computational Tools in Drug Design and Development, Springer Nature Singapore, Singapore. 2025, https://doi.org/10.1007/978-981-96-4154-3.

[20] M.H. Widyananda, S. Puspitarini, A. Rohim, F.A. Khairunnisa, Y.D. Jatmiko, M. Masruri, N. Widodo, Anticancer potential of turmeric (*Curcuma longa*) ethanol extract and prediction of its mechanism through the Akt1 pathway, F1000Research 11 (2022) 1–19, https://doi.org/10.12688/f1000research.75735.1.

[21] A.C. Pushkaran, K. Kumaran, A. Maria T, R. Biswas, C.G. Mohan, Identification of a PD1/PD-L1 inhibitor by structure-based pharmacophore modelling, virtual screening, molecular docking and biological evaluation, Mol. Inform. 42 (2023) 1–16, https://doi.org/10.1002/minf.202200254.

[22] W. Nafisah, F. Fatchiyah, M.H. Widyananda, Y.I. Christina, M. Rifa'i, N. Widodo, M.S. Djati, Potential of bioactive compound of *Cyperus rotundus* L. rhizome extract as inhibitor of PD-L1/PD-1 interaction: an in silico study, Agric. Nat. Resour. 56 (2022) 751–760, https://doi.org/10.34044/j.anres.2022.56.4.09.

[23] B. Robison, S. Diong, A. Kumar, T.M. Moon, O. Chang, B. Chau, C. Bee, I. Barman, A. Rajpal, A.J. Korman, S.M. West, P. Strop, P.S. Lee, Engineered ipilimumab variants that bind human and mouse CTLA-4, mAbs 17 (2025) 1–13, https://doi.org/10.1080/19420862.2025.2451296.

[24] Y. Liu, M. Grimm, W. Dai, M. Hou, Z.-X. Xiao, Y. Cao, CB-Dock: a web server for cavity detection-guided protein–ligand blind docking, Acta Pharmacol. Sin. 41 (2020) 138–144, https://doi.org/10.1038/s41401-019-0228-6.

[25] M.H. Widyananda, F. Fatchiyah, L. Muflikhah, S.M. Ulfa, N. Widodo, Computational examination to reveal Kaempferol as the most potent active compound from *Euphorbia hirta* against breast cancer by targeting AKT1 and ERα, Egypt, J. Basic Appl. Sci. 10 (2023) 753–767, https://doi.org/10.1080/2314808X.2023.2272385.

[26] N. Kumar, P. Mandal, B. Kumar, P. Rani, D.V. Singh, Applications of molecular dynamics simulation and MM-PBSA methods in discovery of veterinary drugs, in: J.-M. Kim, R.K. Pathak, eds., Bioinformatics in Veterinary Science, Springer Nature Singapore, Singapore. 2025, pp. 325–366, https://doi.org/10.1007/978-981-97-7395-4_14.

[27] Y. Guo, J. Tong, J. Liang, K. Shi, X. Song, Z. Guo, B. Liu, J. Xu, Molecular insight into binding affinities and blockade effects of selected flavonoid compounds on the PD-1/PD-L1 pathway, RSC Adv. 14 (2024) 25908–25917, https://doi.org/10.1039/D4RA03877K.

[28] M.M.A. Ezaj, Md. Junaid, Y. Akter, A. Nahrin, A. Siddika, S.S. Afrose, S.M.A. Nayeem, Md.S. Haque, M.A. Moni, S.M.Z. Hosen, Whole proteome screening and identification of potential epitopes of SARS-CoV-2 for vaccine design-an immunoinformatic, molecular docking and molecular dynamics simulation accelerated robust strategy, J. Biomol. Struct. Dyn. 40 (2022) 6477–6502, https://doi.org/10.1080/07391102.2021.1886171.

[29] D. Szklarczyk, R. Kirsch, M. Koutrouli, K. Nastou, F. Mehryary, R. Hachilif, A.L. Gable, T. Fang, N.T. Doncheva, S. Pyysalo, P. Bork, L.J. Jensen, C. von Mering, The STRING database in 2023: protein–protein association networks and functional enrichment analyses for any sequenced genome of interest, Nucleic Acids Res. 51 (2023) D638–D646, https://doi.org/10.1093/nar/gkac1000.

[30] M.H. Widyananda, S.K. Pratama, A.N.M. Ansori, Y. Antonius, V.D. Kharisma, A.A.A. Murtadlo, V. Jakhmola, M. Rebezov, M. Khayrullin, M. Derkho, E. Ullah, R.J.K. Susilo, S. Hayaza, A.P. Nugraha, A. Proboningrat, A. Fadholly, M.T. Sibero, R. Zainul, Quercetin as an anticancer candidate for glioblastoma multiforme by targeting AKT1, MMP9, ABCB1, and VEGFA: an in silico study, Karbala Int. J. Mod. Sci. 9 (2023) 450–459, https://doi.org/10.33640/2405-609X.3312.

[31] A. Daina, O. Michielin, V. Zoete, SwissADME: a free web tool to evaluate pharmacokinetics, drug-likeness and medicinal chemistry friendliness of small molecules, Sci. Rep. 7 (2017) 1–13, https://doi.org/10.1038/srep42717.

[32] D.A. Filimonov, A.A. Lagunin, T.A. Gloriozova, A.V. Rudik, D.S. Druzhilovskii, P.V. Pogodin, V.V. Poroikov, Prediction of the biological activity spectra of organic compounds using the Pass Online Web Resource, Chem. Heterocycl. Compd. 50 (2014) 444–457, https://doi.org/10.1007/s10593-014-1496-1.

[33] N.M. O'Boyle, M. Banck, C.A. James, C. Morley, T. Vandermeersch, G.R. Hutchison, Open Babel: an open chemical toolbox, J. Cheminformatics 3 (2011) 1–14, https://doi.org/10.1186/1758-2946-3-33.

[34] P. García-Manrique, N.D. Machado, M.A. Fernández, M.C. Blanco-López, M. Matos, G. Gutiérrez, Effect of drug molecular weight on niosomes size and encapsulation efficiency, Colloids Surf. B Biointerfaces. 186 (2020) 1–7, https://doi.org/10.1016/j.colsurfb.2019.110711.

[35] P.S. Sobral, V.C.C. Luz, J.M.G.C.F. Almeida, P.A. Videira, F. Pereira, Computational approaches drive developments in immune-oncology therapies for PD-1/PD-L1 immune checkpoint inhibitors, Int. J. Mol. Sci. 24 (2023) 1–28, https://doi.org/10.3390/ijms24065908.

[36] L. Luo, A. Zhong, Q. Wang, T. Zheng, Structure-based pharmacophore modeling, virtual screening, molecular

docking, ADMET, and molecular dynamics (MD) simulation of potential inhibitors of PD-L1 from the Library of Marine Natural Products, Mar. Drugs. 20 (2021) 1–18, https://doi.org/10.3390/md20010029.
[37] A. Madushanka, R.T. Moura, N. Verma, E. Kraka, Quantum mechanical assessment of protein–ligand hydrogen bond strength patterns: insights from semiempirical tight-binding and local vibrational mode theory, Int. J. Mol. Sci. 24 (2023) 1–24, https://doi.org/10.3390/ijms24076311.
[38] Y.-Z. Liu, Y.-N. Chen, Q. Sun, The dependence of hydrophobic interactions on the shape of solute surface, Molecules 29 (2024) 1–24, https://doi.org/10.3390/molecules29112601.
[39] O.M.H. Salo-Ahen, I. Alanko, R. Bhadane, A.M.J.J. Bonvin, R.V. Honorato, S. Hossain, A.H. Juffer, A. Kabedev, M. Lahtela-Kakkonen, A.S. Larsen, E. Lescrinier, P. Marimuthu, M.U. Mirza, G. Mustafa, A. Nunes-Alves, T. Pantsar, A. Saadabadi, K. Singaravelu, M. Vanmeert, Molecular dynamics simulations in drug discovery and pharmaceutical development, Processes 9 (2020) 1–60, https://doi.org/10.3390/pr9010071.
[40] M. Zhang, J. Li, K. Yan, H. Zhou, S. Mei, B. Wang, D. Li, X. Du, M. Liu, P. Zhang, J.K. Fields, L. Ye, P. Zheng, Y. Liu, M.J. Lenardo, Y. Zhang, pH-dependent dissociation from CTLA-4 in early endosomes improves both safety and anti-tumor activity of anti-CTLA-4 antibodies, Proc. Natl. Acad. Sci. 122 (2025) 1–11, https://doi.org/10.1073/pnas.2422731122.
[41] M. Nakhjavani, S. Shigdar, Natural blockers of PD-1/PD-L1 interaction for the immunotherapy of triple-negative breast cancer-brain metastasis, Cancers 14 (2022) 1–16, https://doi.org/10.3390/cancers14246258.
[42] T. Yu, N. Sudhakar, C.D. Okafor, Illuminating ligand-induced dynamics in nuclear receptors through MD simulations, Biochim. Biophys. Acta BBA Gene Regul. Mech. 1867 (2024) 1–9, https://doi.org/10.1016/j.bbagrm.2024.195025.
[43] N. Sobhani, D.R. Tardiel-Cyril, A. Davtyan, D. Generali, R. Roudi, Y. Li, CTLA-4 in regulatory T cells for cancer immunotherapy, Cancers 13 (2021) 1–18, https://doi.org/10.3390/cancers13061440.
[44] A. Dąbrowska, M. Grubba, A. Balihodzic, O. Szot, B.K. Sobocki, A. Perdyan, The role of regulatory T cells in cancer treatment resistance, Int. J. Mol. Sci. 24 (2023) 1–20, https://doi.org/10.3390/ijms241814114.
[45] E. Frijlink, D.M.T. Bosma, J. Busselaar, T.W. Battaglia, M.D. Staal, I. Verbrugge, J. Borst, PD-1 or CTLA-4 blockade promotes CD86-driven Treg responses upon radiotherapy of lymphocyte-depleted cancer in mice, J. Clin. Invest. 134 (2024) 1–15, https://doi.org/10.1172/JCI171154.
[46] M. Mfeka, O. Onisuru, R. Pandian, Y. Sayed, T. Khoza, I. Achilonu, Crystal enigma: understanding diverse protein conformational dynamics, ligand selectivity and interaction in multi-space group crystals using computational modelling, Results Chem. 16 (2025) 1–13, https://doi.org/10.1016/j.rechem.2025.102288.
[47] M. Bouqdayr, A. Abbad, H. Baba, A. Saih, L. Wakrim, A. Kettani, Computational analysis of structural and functional evaluation of the deleterious missense variants in the human *CTLA4* gene, J. Biomol. Struct. Dyn. 41 (2023) 14179–14196, https://doi.org/10.1080/07391102.2023.2178509.
[48] K. Ozvoldik, T. Stockner, E. Krieger, YASARA Model–interactive molecular modeling from two dimensions to virtual realities, J. Chem. Inf. Model. 63 (2023) 6177–6182, https://doi.org/10.1021/acs.jcim.3c01136.
[49] A. Alanzi, A.Y. Moussa, R.A. Mothana, M. Abbas, I. Ali, In silico exploration of PD-L1 binding compounds: structure-based virtual screening, molecular docking, and MD simulation, PLoS One 19 (2024) 1–17, https://doi.org/10.1371/journal.pone.0306804.
[50] Q. Liu, Y. Guan, S. Li, Programmed death receptor (PD-)1/PD-ligand (L)1 in urological cancers: the "all-around warrior" in immunotherapy, Mol. Cancer 23 (2024) 1–26, https://doi.org/10.1186/s12943-024-02095-8.
[51] A. Salminen, The role of the immunosuppressive PD-1/PD-L1 checkpoint pathway in the aging process and age-related diseases, J. Mol. Med. 102 (2024) 733–750, https://doi.org/10.1007/s00109-024-02444-6.
[52] L. Yu, K. Huang, Y. Liao, L. Wang, G. Sethi, Z. Ma, Targeting novel regulated cell death: ferroptosis, pyroptosis and necroptosis in anti-PD -1/PD-L1 cancer immunotherapy, Cell Prolif. 57 (2024) 1–16, https://doi.org/10.1111/cpr.13644.
[53] G.M. Gholam, F.R. Mahendra, R.A.P. Irsal, M.A. Dwicesaria, M. Ariefin, M. Kristiadi, A.F.M. Rizki, W.A. Azmi, I.M. Artika, J.E. Siregar, Computational exploration of compounds in *Xylocarpus granatum* as a potential inhibitor of *Plasmodium berghei* using docking, molecular dynamics, and DFT studies, Biochem. Biophys. Res. Commun. 733 (2024) 1–25, https://doi.org/10.1016/j.bbrc.2024.150684.